Hindawi
Shock and Vibration
Volume 2020, Article ID 8887529, 10 pages
https://doi.org/10.1155/2020/8887529

Research Article

Mechanism Analysis of a Low-Frequency Disc Brake Squeal Based on an Energy Feed-In Method for a Dual Coupling Subsystem

Yidong Wu

GAC Automotive Research & Development Center, Guangzhou 511434, China

Correspondence should be addressed to Yidong Wu; wuyidong@gacrnd.com

Received 13 April 2020; Revised 23 June 2020; Accepted 8 July 2020; Published 28 July 2020

Academic Editor: Marco Lepidi

Brake squeal is a major component of vehicle noise. To explore the mechanism of the low-frequency brake squeal, a finite element model of an automobile disc brake was established, and a complex mode numerical simulation was performed. According to the unstable modes stemming from the complex modal analysis results, the low-frequency range brake squeal can be determined. Based on an energy feed-in method, the coupling subsystems of the piston-caliper and the disc-pad were established, and a calculation formula for the feed-in energy of the dual coupling subsystem was derived. The results showed that when the feed-in energy of the dual coupling subsystem is close to zero, the complex mode cannot be excited at the corresponding frequency. In addition, the difference in feed-in energy between the two coupling subsystems is positively correlated with the probability of the brake squeal, which can be used to determine the complex mode under which the brake squeal may occur. The greater the feed-in energy of a coupling subsystem is, the more likely it is that the maximum brake vibration mode will appear at this subsystem or its adjacent parts. The increase in brake oil pressure will eliminate some lower-frequency sounds but will not change the frequency of the original low-frequency brake squeals.

1. Introduction

In recent years, the problem of automobile brake noise has attracted increasing attention from consumers. Automobile brake noise can be roughly divided into three types: groan, low-frequency squeal, and high-frequency squeal. The corresponding frequencies are 50 Hz~1000 Hz, 1000 Hz~6000 Hz, and above 6000 Hz. Brake squeal is a global problem that has vexed both academia and industry, and there is currently no unified understanding of its generation mechanism [1].

The occurrence of an automobile brake squeal can be considered to have an important relationship with the contact characteristics of the friction pad and the brake disc. Some studies have used the contact surfaces as the research object and proposed the friction characteristic theory and the friction self-locking theory to explain the cause of automobile brake squeals [2–6]. The mechanical behavior of the friction pair has a very significant effect on brake noise. In addition to the disc and the friction pads, the resonance or frictional contact of other parts may also cause a brake squeal [7, 8]. According to the theory of modal coupling self-excited vibration, the brake squeal is caused by the improper matching of the structural parameters of various parts during friction [9–11]. Based on modal coupling theory, complex modal analysis is widely used to reduce the automobile brake squeal. The complex modal analysis method introduces frictional force into the friction pair so that the stiffness matrix of the system becomes asymmetric and generates complex eigenvalues, which can be used to judge the stability of the system and the tendency towards the squeal. With the development of computer technology, complex modal numerical brake simulations of brakes have been widely used in automobile brake squeal research [11–13].

The energy feed-in method proposed by Guan can further elucidate the contact behavior between the brake disc and the friction pads. Changing the chamfering, friction

coefficient, or material parameters of the pads can reduce braking noise [14, 15]. Subsequent studies on the feed-in energy of brakes focused only on a coupling subsystem composed of the disc and the friction pads and ignored the influence of other coupling parts [16, 17]. The study of the brake squeal should consider the feed-in energy of the friction pairs during the whole braking process because the value of feed-in energy will affect the brake squeal amplitude [18, 19]. During the braking process, the oil pressure provides the braking force. There are two main friction pairs with obvious sliding in a braking system: one is the disc-pad friction pair, and the other is the caliper-piston friction pair. Most studies have focused on the former, while the influence mechanism of the latter has been rarely studied in terms of the brake squeal. In fact, as the brake oil pressure changes, the magnitude and frequency of brake squeals may also change accordingly. The brake oil pressure affects not only the frictional force between the disc and pads but also the vibration patterns of the caliper and the piston. Therefore, the concept of a "dual coupling subsystem" is first proposed in this research, which includes a piston-caliper coupling subsystem and a disc-pad coupling subsystem. The feed-in energy expression of the dual coupling subsystem was also derived in this study, which can quantitatively analyze the factors affecting the low-frequency brake squeal and explore the mechanism of the squeal more comprehensively.

This research established a finite element model of automobile disc brakes and carried out complex mode numerical simulations under different brake oil pressures. According to the real part of the complex modal eigenvalue, the low-frequency brake squeal in the range of 1000 Hz ~ 6000 Hz can be found to reproduce the actual squeal situation. Based on the energy feed-in analysis method, the piston-caliper and disc-pad coupling subsystems were established, and an energy feed-in calculation method was derived for this dual coupling subsystem. The influence mechanism of brake oil pressure on the brake squeal was further analyzed by feed-in energy, which provides a theoretical basis for the study of automobile braking noise.

2. Analysis Method

2.1. Complex Mode Characteristic Analysis Method. A finite element discretization was carried out for each part of the braking system, and the equation of motion for the braking system was established as follows:

$$\{M\}\left\{\ddot{U}\right\} + \{C\}\left\{\ddot{U}\right\} + \{K\}\{U\} = \{0\}, \tag{1}$$

where $\{U\}$ is the displacement of discrete nodes and $\{M\}$, $\{C\}$, and $\{K\}$ are the discrete mass matrix, damping matrix, and stiffness matrix, respectively. Due to the existence of frictional force, the stiffness matrix $\{K\}$ is asymmetric, which leads to a complex eigenvalue for the solution of equation (1).

Assuming $\{U\} = \{\psi\}e^{\lambda t}$, substituting it into equation (1), there is

$$\left(\lambda^2\{M\} + \lambda\{C\} + \{K\}\right)\{\psi\} = D(\lambda)\{\psi\} = \{0\}, \tag{2}$$

where $D(\lambda)$ is the eigenmatrix of equation (2) and $\{\psi\}$ is the eigenvector.

The eigenvalue λ can be written in the form of $\lambda = a + i\omega$, where a is the real part of the eigenvalue, representing the damping coefficient, and ω is the imaginary part of the eigenvalue, representing the modal frequency. When $a > 0$, the system is a divergent unstable system. The larger the value of a is, the greater the probability that the system is unstable, and thus a squeal is more likely to occur at this frequency. Therefore, the real part of the eigenvalue is one of the important indicators to determine whether the brake squeal will occur.

2.2. Energy Feed-In Analysis Method. For the brake system, the external energy input is converted into the braking force and driving force. There are obvious relative motions existing in the piston-caliper and disc-pad subsystems. To comprehensively study the brake vibrations, the energy feed-in model of the dual coupling subsystem was established, namely, the piston-caliper coupling subsystem and the disc-pad coupling subsystem. The piston-caliper coupling subsystem was used as an example to derive the calculation method of its feed-in energy.

The occurrence of braking squeals indicates that the system is in an unstable state, which is mainly reflected by the unexpected vibration between the contact surfaces of the structure. The unexpected vibration direction is considered to be perpendicular to the relative motion direction. The relative movement direction of the piston-caliper subsystem is the braking direction, and the relative movement direction of the disc-pad subsystem is the tangential direction of rotation. Therefore, this paper separately considers the feed-in energy perpendicular to the above two directions. It can be considered that the feed-in energy discussed in this research is essentially a disturbance energy to the system.

Figure 1 shows an internal schematic diagram of the piston and the caliper, and the coordinate system in the figure is a global coordinate system. Under the brake oil pressure, the piston and the caliper move along the y-axis.

Nodes A and B are the corresponding nodes of the i-th pair on the piston and the caliper, respectively, which completely coincide before the movement occurs. The contact stiffness between the caliper and the piston is k_1.

The displacements of node A and node B are U_i^p and U_i^c, respectively, in which the superscripts p and c denote the piston and the caliper, respectively. Displacement U_i consists of the vibration mode shapes x_i, y_i, and z_i in three directions. If the forms of motion in all directions are harmonic motions, then

$$\begin{cases} x_i = A_{i(x)}\sin\left(\omega t + \theta_{i(x)}\right), \\ y_i = A_{i(y)}\sin\left(\omega t + \theta_{i(y)}\right), \\ z_i = A_{i(z)}\sin\left(\omega t + \theta_{i(z)}\right). \end{cases} \tag{3}$$

The force and relative displacement between node A and node B in the z direction are as follows:

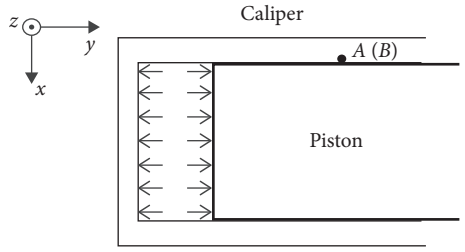

Figure 1: Schematic diagram of the piston-caliper coupling subsystem.

$$F_{i(z)} = k_1\left(z_i^p - z_i^c\right), \tag{4}$$

$$z_i^p - z_i^c = A_{i(z)}^p \sin\left(\omega t + \theta_{i(z)}^p\right) - A_{i(z)}^c \sin\left(\omega t + \theta_{i(z)}^c\right). \tag{5}$$

In a vibration period T, the feed-in energy of node A and node B in the z direction is

$$E_{i(z)}^{p-c} = \int_0^T F_{i(z)}\left(\dot{z}_i^p - \dot{z}_i^c\right)\mathrm{d}t. \tag{6}$$

Substituting equation (4) and (5) into equation (6), we obtain

$$E_{i(z)}^{p-c} = k_1 A_{i(z)}^p A_{i(z)}^c \sin\left(\theta_{i(z)}^p - \theta_{i(z)}^c\right). \tag{7}$$

In the same way, the feed-in energy of node A and node B in the x direction is

$$E_{i(x)}^{p-c} = k_1 A_{i(x)}^p A_{i(x)}^c \sin\left(\theta_{i(x)}^p - \theta_{i(x)}^c\right). \tag{8}$$

Summing the feed-in energy of all relative nodes in the x and z directions, the expression of the feed-in energy E^{p-c} of the piston-caliper coupling subsystem can be obtained as

$$E^{p-c} = \sum_1^n \left(E_{i(x)}^{p-c} + E_{i(z)}^{p-c}\right), \quad i = 1, 2, \ldots, n. \tag{9}$$

For the disc-pad coupling subsystem with contact stiffness k_2, the feed-in energy in the x and y directions is considered in the global coordinate system xyz, so the expression of feed-in energy E^{d-f} of the disc-pad coupling model is as follows:

$$E^{d-f} = \sum_1^n \left(E_{i(x)}^{d-f} + E_{i(y)}^{d-f}\right), \quad i = 1, 2, \ldots, n. \tag{10}$$

From equations (7) and (10), it can be seen that the amplitude and the phase of the discretization node will affect the feed-in energy of the dual coupling subsystem. The amplitudes and phases can be obtained by a finite element numerical simulation; therefore, the energy feed-in analysis method can be combined with the complex mode characteristic analysis method to analyze the brake squeal.

3. Complex Modal Numerical Brake Simulation

3.1. Establishment of Finite Element Brake Model. Based on the phenomenon of the brake squeal at low frequencies, this study undertook a finite element numerical simulation of the brake complex mode. The finite element model of the brake is shown in Figure 2, which consists of the brake disc, friction pads, piston, caliper, caliper bracket, and suspension. The brake model was divided by C3D4 elements, and the average size of which was 2.5 mm (the diameter of the disc was approximately 320 mm). The number of global elements was approximately 1.4 million. To calculate the feed-in energy of the system, the nodes of the contact surface in each coupling subsystem completely coincided. The disc, caliper, bracket, and piston were all regarded as isotropic materials, and the material parameters are shown in Table 1.

The friction pads were anisotropic materials. In the local coordinate system of the friction pads, the x-y plane was parallel to the disc surface. The x direction was the linear speed direction of the brake disc, and the z direction was the normal direction of the friction pad plane. The material parameters of the pads are shown in Table 2.

The surface contact types, contact stiffness, initial clearance, and penetration were all defined. The surface-to-surface contact with friction was mainly used between the components, where the friction coefficient between the disc and the pad was 0.6. The knuckle and the bracket were tied together to prevent relative slippage. In addition, B31 elements were established between the knuckle and the bracket, and pretensioning forces were applied to them to simulate the bolt effect. The magnitude of pretensioning force will affect the contact stiffness and then affect the results of the complex modal analysis. The pretensioning force value depends on the type of bolts. The tightening torque of the bolt measured in the experiment is approximately 120 N m, which is converted into a preload of approximately 40 kN.

3.2. Complex Modal Analysis of Brake and Rationality Verification of Model. Based on the low-frequency brake squeal produced by the bench test of a car at 3050 Hz, an operational definition shape (ODS) test was performed on the brake at this frequency to observe the vibration mode status, and the results were compared with those in the finite element complex mode analysis.

A partial nonlinear perturbation modal analysis is used in the complex modal analysis simulation, and before the complex modal analysis, a nonlinear static analysis was carried out. To make the calculations converge, the pads and the disc were contacted before the movement started, and then the precontact was released while the rotation and the oil pressure were applied. During the loading condition, the oil pressure and disc speed were kept constant. The frequency range was within 7000 Hz.

Under the condition of 0.8 MPa oil pressure, the characteristic frequencies and corresponding real parts of the complex modal simulation were extracted, and the result of this complex modal simulation is plotted in Figure 3. Figure 3 shows that positive real parts appear at frequencies of 1639 Hz, 3030 Hz, and 3983 Hz. The real part at 3030 Hz is the largest, which indicates that the squeal is more likely to occur at this frequency. The vibration mode shapes of the brake system at 3030 Hz were extracted and compared with those in the ODS test. The comparison results are shown in Figure 4. The mode shapes of the caliper, bracket, and

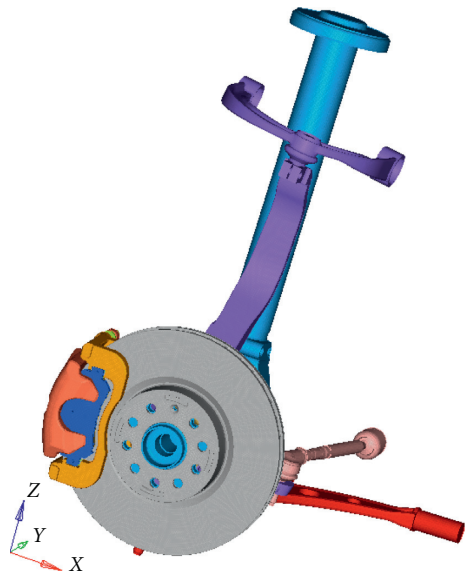

Figure 2: Finite element model of the brake.

Table 1: Material parameters of main parts.

Part	Density (kg/m^3)	Elastic modulus (MPa)	Poisson's ratio
Disc	7.20×10^3	1.20×10^5	0.24
Caliper	7.20×10^3	1.62×10^5	0.30
Bracket	7.20×10^3	1.62×10^5	0.30
Piston	7.85×10^3	2.10×10^5	0.30

Table 2: Material parameters of the pads.

Density (kg/m^3)	$E_x = E_y$ (MPa)	E_z (MPa)	$G_{xz} = G_{yz}$ (MPa)	G_{xz} (MPa)	$\nu_{xz} = \nu_{yz}$	ν_{xz}
2.52×10^3	9.0×10^3	4.0×10^3	2.5×10^3	3.5×10^3	0.36	0.13

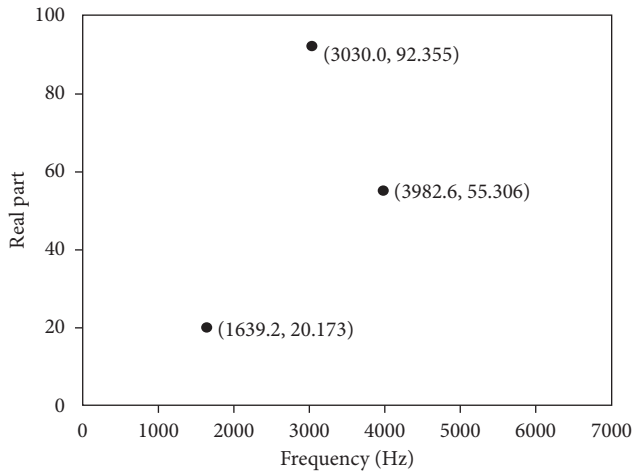

Figure 3: Result of complex modal simulation under 0.8 MPa oil pressure.

support plate in the complex modal simulation at 3030 Hz are almost the same as those in the ODS test at 3050 Hz.

Through the comparison of the real part values at the characteristic frequencies and the mode shapes between the simulation and the test, it is shown that the low-frequency brake squeal can occur near 3000 Hz in the finite element simulation. The squeal of the bench test was reproduced successfully, and the rationality of the finite element model and the material parameters is also verified.

4. Influence Mechanism of Brake Oil Pressure on Brake Squeal

4.1. Complex Modal Analysis Results under Different Brake Oil Pressures. The range of brake oil pressure is set from 0.2 MPa to 1.4 MPa, and the rotation speed of the disc is 1 rad/s. The results of the complex modal analysis of the brake under different brake oil pressures are shown in Figure 5. A total of three complex characteristic frequencies appear under the brake oil pressure in the above range, which are approximately 1600 Hz, 3000 Hz, and 4000 Hz. The vibration mode shapes at the complex characteristic frequencies are shown in Figure 6. The mode shape near 1600 Hz is mainly due to the vibration of the disc, and the maximum shape appears on the support plate of the friction plate at 3000 Hz. At 4000 Hz, the maximum shape appears on the guide pin, which connects the caliper and the bracket.

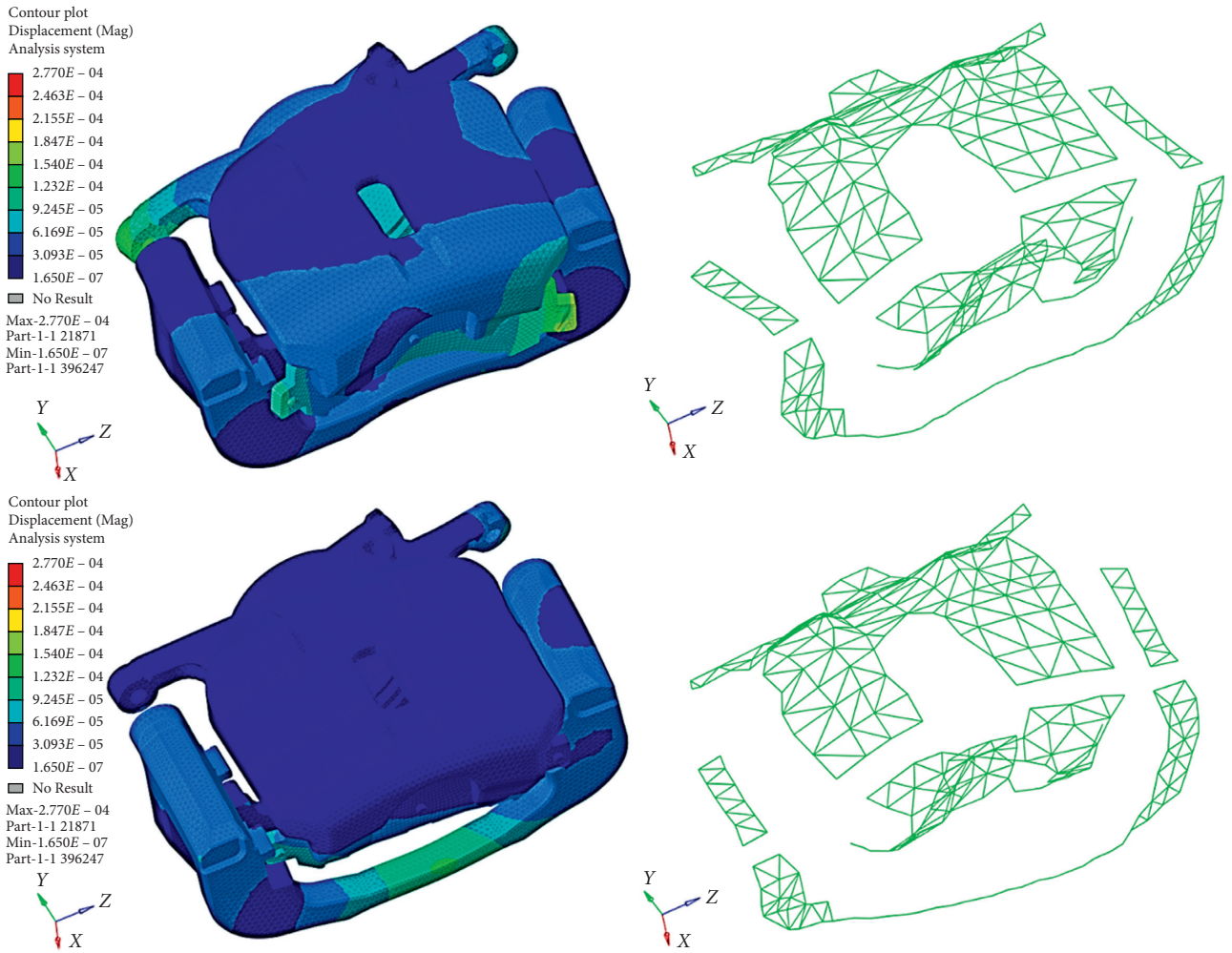

Figure 4: Mode shapes of numerical simulation near 3000 Hz is similar to that of the ODS test.

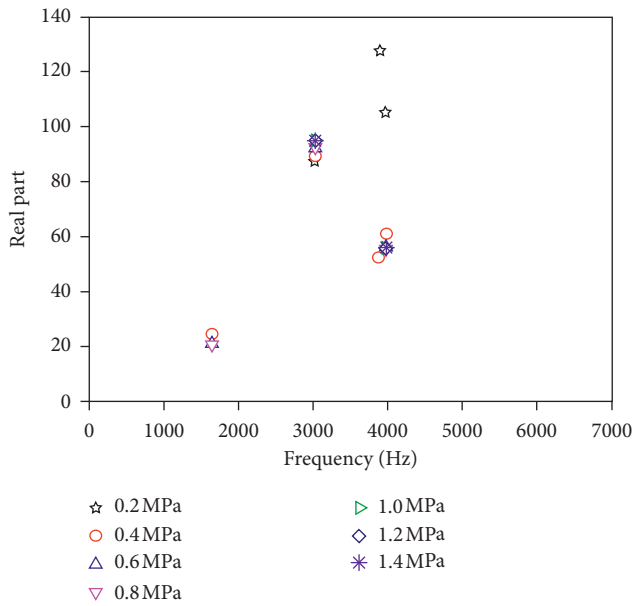

Figure 5: Results of complex modal analysis of the brake under different brake oil pressures.

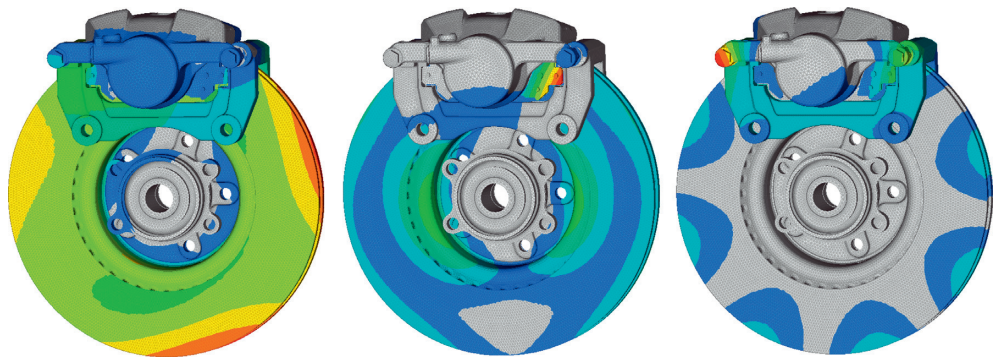

Figure 6: Vibration mode shapes at the complex characteristic frequencies.

To provide more clarity, the loading conditions of brake oil pressure are divided into three grades, namely, low grade (0.2 MPa and 0.4 MPa), medium grade (0.6 MPa and 0.8 MPa), and high grade (1.0 MPa, 1.2 Mpa, and 1.4 MPa). In Figure 5, it can be seen that the low-grade oil pressure will generate two very close complex characteristic frequencies near 4000 Hz, which means that the mode coupling phenomenon will occur, and the brake may generate a 4000 Hz low-frequency brake squeal. All three complex characteristic frequencies occur in the medium-grade brake oil pressure, of which the real part of 3000 Hz is the largest. The high-grade brake oil pressure eliminates the squeal near 1600 Hz, leaving only 3000 Hz and 4000 Hz complex characteristic frequencies. However, the real parts under high-grade oil pressure are basically the same as those under medium-grade oil pressure, indicating that although the increase in brake oil pressure will avoid some lower-frequency noise, it will not change the frequency of the original low-frequency brake squeals.

4.2. Feed-In Energy of Brakes under Different Brake Oil Pressures. There are 588 pairs of nodes in the piston-caliper coupling subsystem and 4260 pairs of nodes in the disc-pad coupling subsystem. The number of nodes in the dual coupling subsystem used to calculate the feed-in energy is sufficient to ensure the accuracy of the calculation results. Abu Bakar and Ouyang [20] proposed a range of different interface coupling stiffness values. It is considered that the coupling stiffness of the two substructure interfaces with strict restrictions on the movement in all directions is larger, while the coupling stiffness between the two substructures with intermittent contact is smaller. Based on the local contact stiffness of the material [21], in this paper, the coupling stiffness of the piston-caliper coupling subsystem was set as $1 \times 10^{10}\ N/m$ and that of the disc-pad coupling subsystem was set as $5 \times 10^{8}\ N/m$. Since $A^{p}_{i(z)}$ and $A^{c}_{i(z)}$ in equation (7) had been normalized, the feed-in energy E can be regarded as the feed-in energy per unit area, and its unit was N/m. Under different brake oil pressures, the values of feed-in energy of the dual coupling subsystem near 1600 Hz and 3000 Hz are shown in Tables 3 and 4, respectively.

It can be seen in Tables 3 and 4 that near 1600 Hz and 3000 Hz, the feed-in energies of the piston-caliper coupling subsystem are always smaller than those of the disc-pad coupling subsystem, which indicates that the disturbance of external energy input to the contact interface between the brake disc and friction pads is more obvious at this time, and the maximum vibration shape of the brake will appear on the disc-pad coupling subsystem or its adjacent parts. In

Table 3: Feed-in energy of the dual coupling subsystem near 1600 Hz.

Pressure	Frequency (Hz)	Real part	Coupling system	Energy (N/m)
0.2	1650.6	/	Piston-caliper	3.54×10^{-11}
			Disc-plate	5.76×10^{-10}
0.4	1641.2	24.023	Piston-caliper	576.49
			Disc-plate	850.00
0.6	1639.2	21.266	Piston-caliper	956.09
			Disc-plate	1100.00
0.8	1639.2	20.173	Piston-caliper	939.16
			Disc-plate	1050.00
1.0	1638.2	/	Piston-caliper	8.35×10^{-10}
			Disc-plate	2.73×10^{-8}
1.2	1638.5	/	Piston-caliper	1.32×10^{-10}
			Disc-plate	4.29×10^{-9}
1.4	1638.5	/	Piston-caliper	9.39×10^{-11}
			Disc-plate	2.37×10^{-9}

Table 4: Feed-in energy of the dual coupling subsystem near 3000 Hz.

Pressure	Frequency (Hz)	Real part	Coupling system	Energy (N/m)
0.2	3024.5	87.619	Piston-caliper	143.39
			Disc-plate	468.08
0.4	3031.5	89.355	Piston-caliper	400.63
			Disc-plate	1500.00
0.6	3032.3	92.141	Piston-caliper	492.25
			Disc-plate	1700.00
0.8	3033.0	92.355	Piston-caliper	531.85
			Disc-plate	1900.00
1.0	3032.3	94.732	Piston-caliper	758.02
			Disc-plate	3100.00
1.2	3032.6	94.844	Piston-caliper	798.88
			Disc-plate	3350.00
1.4	3032.9	94.825	Piston-caliper	845.52
			Disc-plate	3700.00

Table 5: Feed-in energy of the dual coupling subsystem near 4000 Hz.

Pressure (MPa)	Frequency (Hz)	Real part	Coupling system	Energy (N/m)
0.2	3972.1	105.13	Piston-caliper	232.67
			Disc-plate	179.49
0.4	3985.0	61.106	Piston-caliper	155.99
			Disc-plate	135.76
0.6	3983.3	56.060	Piston-caliper	164.12
			Disc-plate	130.18
0.8	3982.6	55.306	Piston-caliper	154.57
			Disc-plate	133.30
1.0	3982.0	55.654	Piston-caliper	147.25
			Disc-plate	123.55
1.2	3982.0	55.765	Piston-caliper	147.48
			Disc-plate	125.15
1.4	3982.1	55.986	Piston-caliper	147.63
			Disc-plate	126.18

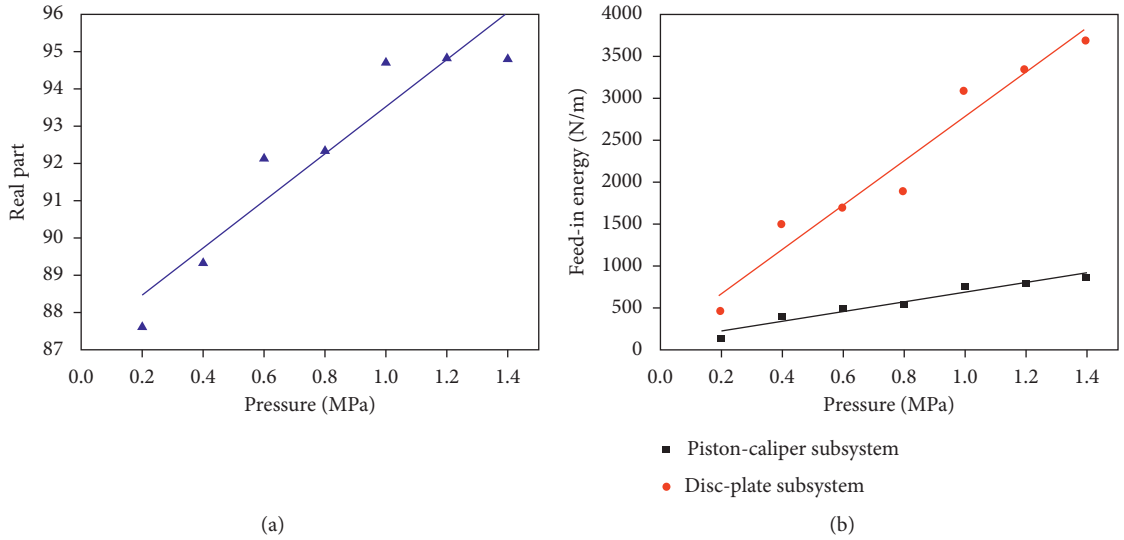

Figure 7: Relationships between brake oil pressure, real part, and feed-in energy at 3000 Hz. (a) Linear relationship between brake oil pressure and the real part. (b) Linear relationship between brake oil pressure and feed-in energy.

addition, from the real part data in Table 3 (pressure of 0.2 MPa, 1.0 MPa, 1.2 Mpa, and 1.4 MPa), it can be seen that when the feed-in energy of the dual coupling subsystem is close to 0, the complex characteristic frequency cannot be excited. Therefore, the feed-in energy reaching a certain threshold is the premise of a low-frequency brake squeal.

Under different brake oil pressures, the feed-in energy values of the dual coupling subsystem near 4000 Hz are shown in Table 5.

Near 4000 Hz, the feed-in energies of the piston-caliper coupling subsystem are always larger than those of the disc-pad coupling subsystem under different oil pressures. The maximum vibration shape of the brake will appear on the piston-caliper coupling subsystem or its adjacent parts. Overall, the greater the feed-in energy of a coupling subsystem is, the more likely the maximum vibration mode of the brake will appear at this subsystem or its adjacent parts, which is consistent with the vibration situation of the parts at different complex characteristic frequencies shown in Figure 6.

4.3. Relationship between Brake Oil Pressure, Real Part, and Feed-In Energy. At the complex characteristic frequencies of 3000 Hz and 4000 Hz, the relationships between brake oil pressure, real part, and feed-in energy are shown in Figures 7 and 8, respectively. When the maximum mode shape appears on the piston-caliper coupling subsystem (3000 Hz), the complex real part and the feed-in energy increase with increasing brake oil pressure, and each variable presents a linear relationship with the brake oil pressure. Though the maximum mode shape appears on the disc-pad coupling subsystem (4000 Hz), the above variables decrease as the oil pressure rises, and each variable and the oil pressure exhibit a power function relationship.

As shown in Figures 7(a) and 8(a), under the same brake oil pressure, the complex characteristic real parts at 3000 Hz are larger than those at 4000 Hz. The difference between the two increases with increasing oil pressure, which makes the brake more likely to produce a 3000 Hz brake squeal. The cause of the above phenomenon can be explained from the perspective of the feed-in energy of the brake. Figures 7(b)

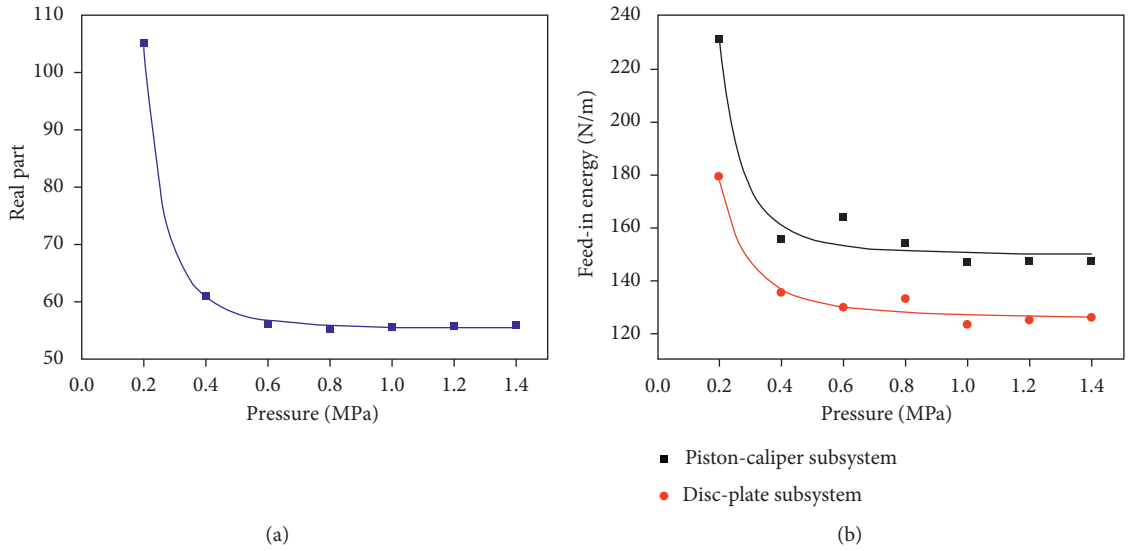

Figure 8: Relationships between brake oil pressure, real part, and feed-in energy at 4000 Hz. (a) Power function relationship between brake oil pressure and the real part. (b) Power function relationship between brake oil pressure and feed-in energy.

and 8(b) show that as the brake oil pressure increases, the feed-in energies of the dual coupling subsystem increase at 3000 Hz, while those at 4000 Hz are almost unchanged. With the increase in the feed-in energy, the mode shape of the coupling system is larger, so the braking noise is more easily generated.

According to the traditional feed-in energy analysis theory, the greater the feed-in energy of the disc-pad coupling subsystem, the easier it is to produce a brake squeal at this frequency. However, under a brake oil pressure of 0.2 MPa, the maximum feed-in energy of the disc-pad subsystem is 3000 Hz, but the system may produce a 4000 Hz squeal, as shown in Tables 4 and 5 and Figure 5. To further determine which complex mode is more likely to produce a brake squeal, it is necessary to explore the relationship between the real part and the feed-in energy. Introducing the relative feed-in energy $\overline{E}$, the expression is as follows:

$$\overline{E} = \frac{E^{d-f} - E^{p-c}}{E^{d-f}}. \tag{11}$$

The variable $\overline{E}$ reflects the feed-in energy relationship between the piston-caliper and the disc-pad coupling subsystems, which can effectively avoid the calculation deviation caused by the contact stiffness error of the coupling subsystem. The relationship between the real part and the relative feed-in energy at each complex characteristic frequency in all oil pressures is shown in Figure 9. The red star symbol represents the real part of the maximum value under each oil pressure, which also represents the maximum probability of the squeal, and the black triangle symbol represents the other complex real parts.

$$R = 258.7\overline{E}^2 - 110.8\overline{E} + 30.3. \tag{12}$$

A quadratic function of formula (12) is used to describe the relationship between the relative feed-in energy and the real part. The dotted line in Figure 9 is at $\overline{E} = 0$. The left side

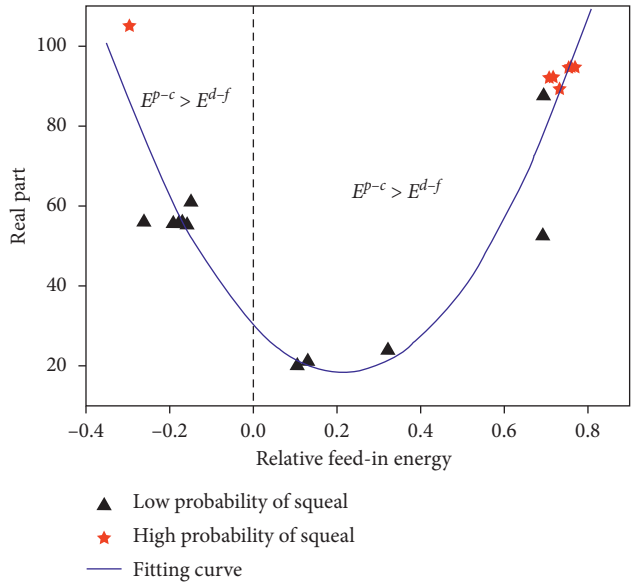

Figure 9: Relationship between the complex real part and the relative feed-in energy.

of the dotted line indicates that the feed-in energy of the piston-caliper coupling subsystem is larger than that of the disc-pad subsystem, and the right side indicates the opposite situation. As the relative feed-in energy increases, the real part increases first and then decreases, and the real parts of the squeal are distributed at both ends of the curve, which shows that the difference in feed-in energy between the two coupling subsystems is positively correlated with the probability of the brake squeal. This can explain why the 4000 Hz brake squeal is more likely to occur under the brake oil pressure of 0.2 MPa. At 3000 Hz, the feed-in energy of the piston-caliper coupling subsystem is small and the feed energy of the disc-pad subsystem is large. According to

equation (11), the value of the relative feed-in energy brake is small. At 4000 Hz, the feed-in energy of the piston-caliper coupling subsystem is larger than that of the disc-pad subsystem, which results in a large relative feed-in energy, so it is easier to produce a squeal at this frequency.

The difference between the feed-in energy of the piston-caliper coupling subsystem and the disc-pad coupling subsystem can be used to determine in which complex mode the brake squeal may occur, which provides a theoretical basis for the recurrence of the brake squeal phenomenon during the bench test.

5. Conclusion

In this study, a finite element model of an automobile disc brake was established, and a complex modal numerical simulation under different brake oil pressures was performed. Two coupling subsystems of the piston-caliper and the disc-pad were established, and the energy feed-in calculation method of the dual coupling subsystem was derived. Based on the complex mode analysis and energy feed-in analysis, the mechanism of the low-frequency squeal of the brake was explored. The main conclusions are as follows:

(1) The larger the real part of the complex feature is, the more likely the brake will produce a brake squeal at this frequency. The increase in brake oil pressure will eliminate some lower-frequency sounds, but will not change the frequency of the original low-frequency brake squeals.

(2) The feed-in energy of the brake is related to the amplitude and the phase of each node in the dual coupling subsystem. The greater the feed-in energy of a coupling subsystem, the maximum vibration mode of the brake will appear at this subsystem or its adjacent parts.

(3) When the maximum mode shape appears on the piston-caliper coupling subsystem, the complex real part and the feed-in energy increase with increasing brake oil pressure, and each variable presents a linear relationship with the brake oil pressure. Though the maximum mode shape appears on the disc-pad coupling subsystem, the above variables decrease as the oil pressure rises, and each variable and the oil pressure exhibit a power function relationship.

(4) Feed-in energy reaching a certain threshold is the premise of the low-frequency brake squeal. The difference in feed-in energy between the two coupling subsystems is positively correlated with the probability of the brake squeal, which can be used to determine under which complex mode the brake squeal may occur.

Data Availability

The data used to support the findings of this study are available from the corresponding author upon request.

Conflicts of Interest

The author declares that there are no conflicts of interest regarding the publication of this paper.

Acknowledgments

This study was supported by the GAC Automotive Research and Development Center (Project no. X2N-DP-9).

References

[1] N. M. Kinkaid, O. M. O'Reilly, and P. Papadopoulos, "Automotive disc brake squeal," *Journal of Sound and Vibration*, vol. 267, no. 1, pp. 105–166, 2003.

[2] J. E. Mottershead, "Vibration- and friction-induced instability in disks," *The Shock and Vibration Digest*, vol. 30, no. 1, pp. 14–31, 1998.

[3] S. Qiao and R. A. Ibrahim, "Stochastic dynamics of systems with friction-induced vibration," *Journal of Sound & Vibration*, vol. 223, no. 1, pp. 115–140, 1999.

[4] R. A. Ibrahim, S. Madhavan, S. L. Qiao, and W. K. Chang, "Experimental investigation of friction-induced noise in disc brake systems," *International Journal of Vehicle Design*, vol. 23, no. 3/4, pp. 218–240, 2000.

[5] C. Cantoni, R. Cesarini, G. Mastinu et al., "Brake comfort-a review," *Vehicle System Dynamics*, vol. 47, 2009.

[6] N. M. Ghazaly, I. Ahmed, and M. El-Sharkawy, "A review of automotive brake squeal mechanisms," *Journal of Mechanical Design & Vibration*, vol. 1, no. 1, pp. 5–9, 2014.

[7] L. H. T. Huynh, A. Dittrich, and O. Dráb, "Model predict vibration and noise of disc brake," *Applied Mechanics and Materials*, vol. 232, pp. 461–464, 2012.

[8] T. Nakae, A. T. Ryu, and T. Y. InoueNakano, "Squeal and chatter phenomena generated in a mountain bike disc brake," *Journal of Sound and Vibration*, vol. 330, no. 10, pp. 2138–2149, 2011.

[9] V. P. Sergienko and S. N. Bukharov, "Vibration and noise in brake systems of vehicles. Part 2: theoretical investigation techniques," *Journal of Friction and Wear*, vol. 30, no. 3, pp. 216–226, 2009.

[10] Y. Du and Y. Wang, "Squeal analysis of a modal-parameter-based rotating disc brake model," *International Journal of Mechanical Sciences*, vol. 131, 2017.

[11] S. Nacivet and J.-J. Sinou, "Modal amplitude stability analysis and its application to brake squeal," *Applied Acoustics*, vol. 116, pp. 127–138, 2017.

[12] J. Kang, "Finite element modelling for the investigation of in-plane modes and damping shims in disc brake squeal," *Journal of Sound and Vibration*, vol. 331, no. 9, pp. 2190–2202, 2012.

[13] C. Kim and K. Zhou, "Analysis of automotive disc brake squeal considering damping and design modifications for pads and a disc," *International Journal of Automotive Technology*, vol. 17, no. 2, pp. 213–223, 2016.

[14] D. Guan and J. Huang, "The method of feed-in energy on disc brake squeal," *Journal of Sound and Vibration*, vol. 261, no. 2, pp. 297–307, 2003.

[15] D. Guan, Y. Du, and X. Wang, "Effect of pad shapes on high-frequency disc brake squeal," *International Journal of Vehicle Design*, vol. 72, no. 4, p. 354, 2016.

[16] N. J. Martin and J. L. Rice, "Examining the use of concept analysis and mapping software for renewable energy feed-in tariff design," *Renewable Energy*, vol. 113, pp. 211–220, 2017.

[17] H. Lyu, J. W. Stephen, C. Chen et al., "Analysis of friction-induced vibration leading to brake squeal using a three degree-of-freedom model," *Tribology Letters*, vol. 65, no. 3, p. 105, 2017.

[18] L. Zhang, K. Diao, D. Meng et al., "Time-varying characteristics of frictional squeal in pin-on-disc system: generation mechanism and key impact factors," *Journal of Mechanical Engineering*, vol. 49, no. 14, pp. 99–105, 2013.

[19] L. Zhang, W. Li, and D. Meng, "Influence of heterogeneous contact stiffness and heterogeneous friction coefficient on frictional squeal," *Shock and Vibration*, vol. 2018, Article ID 6379201, 21 pages, 2018.

[20] A. R. Abu Bakar and H. Ouyang, *Recent Studies of Car Disc Brake Squeal*, Nova Science Publishers, Hauppauge, NY, USA, 2008.

[21] F. Chen, "Disc brake squeal: an overview," *International Journal of Vehicle Design*, vol. 51, 2007.